JCTC Journal of Chemical Theory and Computation

ARTICLE

pubs.acs.org/JCTC

# RASPT2/RASSCF vs Range-Separated/Hybrid DFT Methods: Assessing the Excited States of a Ru(II)bipyridyl Complex

Daniel Escudero[†] and Leticia González*[,‡]

Institut für Physikalische Chemie, Friedrich-Schiller Universität, Helmholtzweg, 4, 07743 Jena, Germany

Supporting Information

**ABSTRACT:** The excited states of the *trans*(Cl)-Ru(bpy)$Cl_2(CO)_2$ (bpy = bypyridyl) transition-metal (TM) complex are assessed using the newly developed second-order perturbation theory restricted active space (RASPT2/RASSCF) method. The delicate problem of partitioning the RAS subspaces (RAS1, RAS2, and RAS3) is addressed, being the choice of the RAS2 the bottleneck to obtain a balanced description of the excited states of different nature when TMs are present. We find that the RAS2 should be composed by the correlation orbitals involved in covalent metal−ligand bonds. The level of excitations within the RAS1 and RAS3 subspaces is also examined. The performance of different flavors of time-dependent density functional theory including pure, hybrid, meta-hybrid, and range-separated functionals in the presence of solvent effects is also evaluated. It is found that none of the functionals can optimally describe all the excited states simultaneously. However, the hybrid M06, B3LYP, and PBE0 functionals seem to be the best compromise to obtain a balanced description of the excited states of *trans*(Cl)-Ru(bpy)$Cl_2(CO)_2$, when comparing with the experimental spectrum. The conclusions obtained in this molecule should pave the road to properly treat excited states of larger Ru−polypyridyl complexes, which are of particular interest in supramolecular chemistry.

## 1. INTRODUCTION

Ru(II) polypyridyl complexes and related compounds are promising candidates as light-harvesting antennas in hot research areas, such as artificial photosynthesis,[1] light-driven catalysis (i.e., sunlight driven splitting of water),[2] or dye-sensitized solar cells (DSSCs),[3] due to a combination of optimal chemical, electrochemical, and photophysical properties. The identification and characterization of the lowest-lying excited states are therefore a challenging task of paramount importance to guide the design of molecular functional materials. To get an insight into the photophysical properties of these complexes, the use of accurate ab initio multiconfiguration methods, as for example, the well-established second-order perturbation theory complete active space[4] (CASPT2/CASSCF) protocol, is highly desirable. Due to the extensive size of such transition-metal (TM) complexes and the need of large active spaces able to handle all the static correlation, such calculations are yet pretty much at the limit of the current computational resources and not very much extended.[5] To our knowledge, there are only a few examples of CASPT2/CASSCF studies on TM−polypyridyl complexes, e.g., on $[Fe(bpy)_3]^{2+}$ [6] or [Re(bpy)(*t*-stpy)]$^{+}$.[7] Despite the considerable effort involved in these studies, they involve reduced CAS reference wave functions with active spaces that might not be extensive enough to account for all the desired correlation effects. The restricted active space method (RASSCF)[8] and its PT2 extension (RASPT2)[9] are very appealing because they allow using considerably larger active spaces than the CASPT2/CASSCF protocol. However, due to the three different partitions of the active space, a number of open questions can be raised regarding its systematic use. In particular, it is not straightforward how the active orbitals in the RAS subspaces should be best distributed or at which level of excitation the results can be considered converged. Recently, Gagliardi and co-workers have performed an extensive number of RASPT2/RASSCF calculations mainly in organic dyes,[10,11] clearly illustrating that the selection of the RAS spaces requires careful calibration. In the case of simple oligomeric $\pi$-conjugated systems, the computationally cheapest strategy is leaving the RAS2 empty while allowing for single, double, triple, and quadruple (SDTQ) excitations within the RAS1 and RAS3 subspaces. This simple recipe allows for an accurate description of ionization potentials and lowest-lying excited states of many organic systems,[10] but unfortunately it cannot be extrapolated to more complicated systems, neither of organic character, like free base porphins,[11] nor of inorganic nature, like Cu(I)-$\alpha$-ketocarboxylate complexes.[12] From this perspective, there is an urge to calibrate the RASSCF approach in TM complexes which otherwise are typically treated by means of density functional theory (DFT) and its time-dependent version (TD-DFT).[13]

The compromise between low computational cost and accuracy obtained with DFT is in general remarkable, and therefore a huge number of ground-state studies for TM complexes are found in the literature.[14] The success of DFT describing ground-state properties is however not comparable to the success of TD-DFT for the study of excited states. TD-DFT is known to have difficulties in describing Rydberg states, charge-transfer (CT) excitations[15] as well as doubly or highly excited states.[16] Attempts to improve the description of CT and Rydberg excitations, while maintaining good quality for local excitations, has led to the development of hybrid functionals with intermediate percentage of exact exchange, such as PBE0,[17] and range-separated hybrid functionals, such as LC-$\omega$PBE[18] or CAM-B3LYP,[19] which have been shown to perform reasonably well describing CT of organic dyes.[20] CT events are common in TM spectroscopy; however, more challenging is that the calculation of the UV−vis spectra of

**Received:** September 13, 2011
**Published:** November 09, 2011

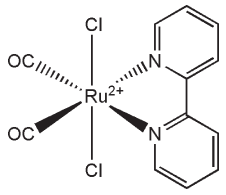


1

**Figure 1.** Chemical structure of *trans*(Cl)-Ru(bpy)$Cl_2(CO)_2$, complex **1**.

complex TM systems also requires the simultaneous balanced description of additional intraligand (IL) and d−d transitions, which are both local excitations. Despite these difficulties, TD-DFT is indiscriminately employed due to its simplicity and apparent black-box behavior, in particular for large systems such as Ru(II) polypyridyl complexes,[21] which are otherwise out of reach from more accurate ab initio methods. Few examples are found in the literature assessing the performance of TD-DFT on TM complexes.[22] However, to our knowledge, there is no evaluation of the performance of hybrid vs range-separated functionals to describe the excited states of TM−polypyridyl and related complexes.

In this contribution we present a RASPT2/RASSCF study of the electronically excited states of *trans*(Cl)-Ru(bpy)$Cl_2(CO)_2$ for which experimental data are available for comparison.[23,24] This complex serves as an example of this general class of systems. It displays different types of excited states and thus represents a challenge for computational chemistry. Different partition schemes of the RAS subspaces (RAS1, RAS2 and RAS3) as well as the level of excitations in the RAS1 and RAS3 subspaces are evaluated. The conclusions reached with this molecular system will provide hints about how to study similar TM compounds, therefore, extending the possibilities of RASPT2/RASSCF to larger TM−polypyridyl complexes. Additionally, and based on the experimental results, the performance of TD-DFT using different functionals in solution is analyzed. Particularly, the behavior of several hybrid, meta-hybrid, pure, and long-range corrected functionals in describing the different types of excitations present in TM complexes is examined and discussed. The conclusions should help to make an adequate choice of the functional when studying very large TM−polypyridyl complexes that cannot be treated within the RASPT2/RASSCF protocol.

## 2. COMPUTATIONAL DETAILS

The *trans*(Cl)-Ru(bpy)$Cl_2(CO)_2$ complex **1** (see Figure 1) was optimized in its electronic ground state under the $C_{2v}$ symmetry constraint at the B3LYP/6−31G* level of theory. Relativistic effects in the Ru atom were considered using the ECP-28-mwb pseudopotential.[25] The complex has been characterized as a true minimum by calculating the Hessian at the same level of theory.

Single point CASPT2/CASSCF and RASPT2/RASSCF calculations were performed on the $C_{2v}$ geometry. These calculations were done with the ANO-rcc-VTZP basis set.[26] Scalar relativistic effects were considered using a standard second-order Douglas−Kroll−Hess (DKH) Hamiltonian.[27] Cholesky decomposition of the electron repulsion integral matrix[28] was used, then reducing the computational times and the disk storage needs. In the CAS calculations, the traditional notation is used, namely CAS($n$,$j$), where $n$ is the number of electrons included in the active space and $j$ is the number of active orbitals. In the RAS calculations, the RAS($n$,$l$,$m$;$i$,$j$,$k$) notation is employed, where $n$ is the number of active electrons, $l$ the maximum of holes in the RAS1, $m$ the maximum of electrons in RAS3, and $i$, $j$, and $k$ the number of orbitals in RAS1, RAS2, and RAS3, respectively.

The choice of the active orbitals for the CASSCF/RASSCF calculations is made in terms of the standard rules for TM compounds.[29,30] Important correlation effects due to the covalency of the Ru metal−ligand bonds via $\sigma$- and $\pi$-bonding interactions are considered by including some relevant $\sigma$ orbitals involving the Ru atom and also the chlorine atoms ($n_{Cl}$−$a_1$ orbital) or the bpy and the CO ligands ($\sigma_{CO\text{-}bpy}$ orbitals, in Figure 2). Relevant $\pi$-bonding interactions are taken into account by including $\pi^*_{CO}$ orbitals and lone pairs of the chlorines atoms ($n_{Cl}$−$b_1$ orbital). In principle we follow the advice given by Pierloot[31] that all orbitals with an important contribution of d character should be included in the active space. Since Ru is a 4d atom, the "double-shell" effect is not as indispensable as for 3d atoms; therefore, this external shell is not considered here for the sake of computational saving. In some sense, these correlation effects are partially recovered upon inclusion of other orbitals, such as the $\pi^*_{CO}$ orbitals, which possess some contribution of 5d character. The intershell effects, i.e., those due to semicore electrons, are very important for the 4d and 5d series, and thus they have been inherently considered by using the ANO-rcc basis set that is optimized to include such correlation effects. Other valence orbitals, such as the $\pi_{CO}$ orbitals and some $\pi_{bpy}/\pi^*_{bpy}$ orbital pairs, are not included in our calculations since a full valence electron treatment is out of reach for CASPT2 and even for RASPT2 calculations in the complex **1**. One strategy followed here is to include many of the orbitals that in principle contribute to static correlation but to a lesser extent, in the RAS1 and RAS3 subspaces, while RAS2 includes the indispensable orbitals involved in the main excited states (low- and high-lying) of **1**; these are the five 4d orbitals and the $\pi_{bpy}/\pi^*_{bpy}$ orbitals. These orbitals are involved in the main metal-centered (MC), metal-to-ligand charge transfer (MLCT) and IL states of **1**. An additional strategy is to include the relevant orbitals involved in the main electronic excitations within the RAS1/3 subspaces, while the correlation orbitals, i.e., those participating in the covalency of the Ru metal−ligand bonds via $\sigma$- and $\pi$-bonding interactions, will be part of the RAS2 subspace, since the correlation orbitals are essential to recover static correlation on the zeroth-order wave function. All the relevant orbitals are depicted in Figure 2.

Specifically, the following subspaces were constructed:

(i) Small CAS active space. It is composed of the five 4d orbitals of the Ru atom and a balanced set of four frontier $\pi_{bpy}/\pi^*_{bpy}$ pair of orbitals, see Figure 2. This active space is used in the CASSCF(14,13) calculations.

(ii) Inclusion of correlation effects to the small CAS active space. A relevant $n_{Cl}$ orbital with important $\sigma$ character, involving lone pairs of the chlorine and the Ru center (see $n_{Cl}$−$a_1$ in Figure 2) as well as two $\pi^*_{CO}$ orbitals ($\pi^*_{CO}$−$b_1$ and $\pi^*_{CO}$−$a_2$) are included in the active space through the RAS1 and RAS3 subspaces. Such selection was made in terms of the higher metal d contributions of such orbitals. Additionally, a pair of $\pi_{bpy}/\pi^*_{bpy}$ orbitals (namely the $\pi_{bpy}$−$2a_2/\pi^*_{bpy}$−$2a_2$ orbitals, see Figure 2) is shifted to the RAS1 and RAS3 subspaces, respectively, because the corresponding occupation numbers were higher/lower than 1.95/0.05. This active space is used in the RASSCF(16,2,2;2,11,3),

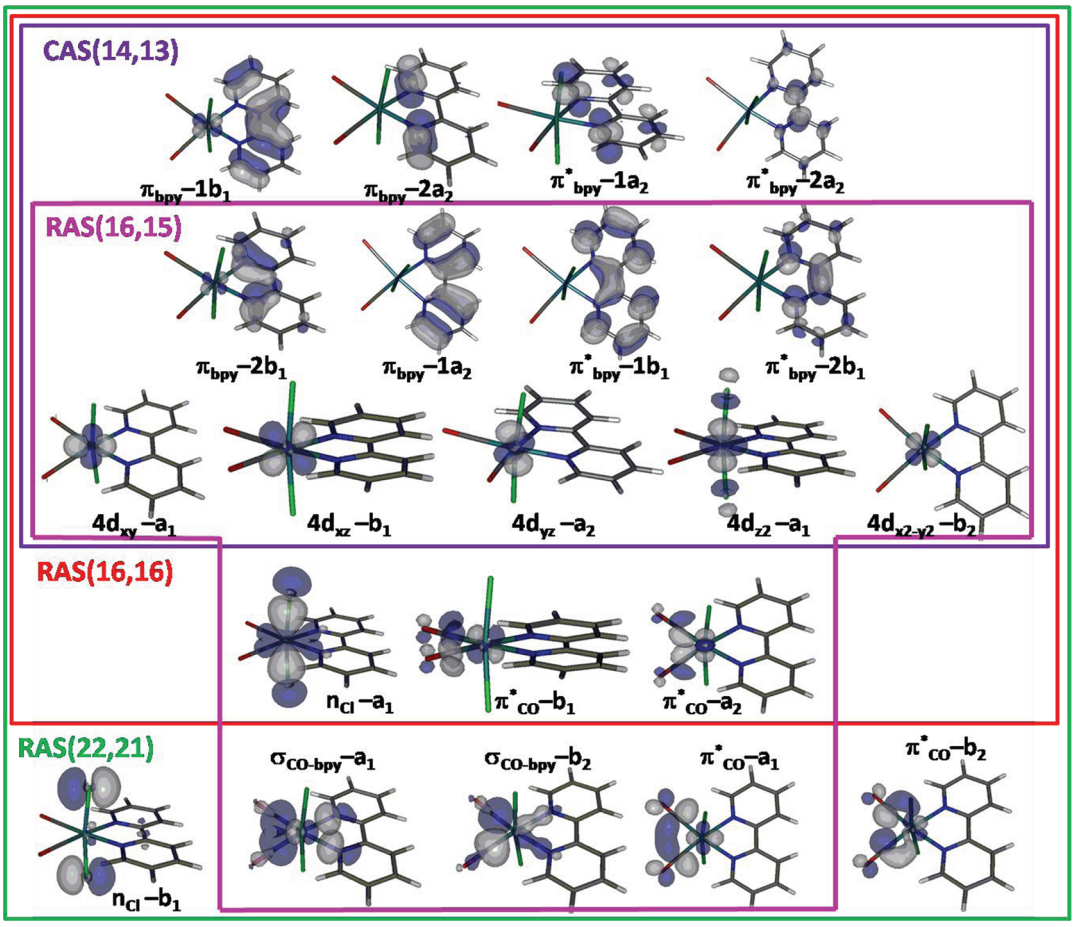


**Figure 2.** CASSCF and RASSCF active spaces employed.

RASSCF(16,3,3;2,11,3), and RASSCF(16,3,4;2,11,3) calculations. For comparison, a calculation where the RAS2 subspace is empty and all the active orbitals are assigned to the RAS1 and RAS3 subspaces is also performed, RASSCF(16,4,4;8,0,8). For the same reason as before, an additional pair of $\pi_{bpy}/\pi^*_{bpy}$ orbitals (namely the pair $\pi_{bpy}-1b_1/\pi^*_{bpy}-1a_2$) was moved into the RAS1/3 subspaces, leading to the RASSCF(16,2,2;3,9,4) calculation.

(iii) Additional correlation effects: Based on the RASSCF(16,2,2;3,9,4) active space, additional correlation orbitals were considered. Again, such selection was done paying attention to the metal d contribution of the included orbitals: In the RAS1 an additional $n_{Cl}$ orbital ($n_{Cl}-b_1$) and two $\sigma_{CO\text{-}bpy}$ orbitals ($\sigma_{CO\text{-}bpy}-a_1$ and $\sigma_{CO\text{-}bpy}-b_2$) were included, and the two remaining $\pi^*_{CO}$ orbitals ($\pi^*_{CO}-a_1$ and $\pi^*_{CO}-b_2$) were put in the RAS3 (see Figure 2). In these calculations the two $\pi_{bpy}/\pi^*_{bpy}$ orbital pairs, $\pi_{bpy}-2a_2/\pi^*_{bpy}-2a_2$ and $\pi_{bpy}-1b_1/\pi^*_{bpy}-1a_2$, were maintained in the RAS1/3 subspaces because they do not play a role in the low- and high-lying excited states. This partition leads to a RASSCF(22,2,2;6,9,6) calculation.

(iv) $\sigma-\pi$ correlation effects in RAS2: Based on the assumption that correlation orbitals should be included in the RAS2 subspace, this subspace is composed by the $n_{Cl}$ orbital ($n_{Cl}-b_1$), two $\sigma_{CO\text{-}bpy}$ orbitals ($\sigma_{CO\text{-}bpy}-a_1$ and $\sigma_{CO\text{-}bpy}-b_2$) and three $\pi^*_{CO}$ orbitals ($\pi^*_{CO}-b_1$, $\pi^*_{CO}-a_2$, and $\pi^*_{CO}-a_1$). Since the occupied $a_1$ orbitals were partially mixed among them, also the $4d_{xy}-a_1$ orbital was included into the RAS2. The rest of 4d orbitals and only the relevant $\pi_{bpy}/\pi^*_{bpy}$ orbital pairs, namely $\pi_{bpy}-2b_1/\pi_{bpy}-1a_2$ and $\pi^*_{bpy}-1b_1/\pi^*_{bpy}-2b_1$, were included in the RAS1 and RAS3 subspaces, allowing up to SDT excitations. This partition leads to a RASSCF(16,3,3;4,7,4) calculations.

The CASSCF/RASSCF calculations presented herein are done as state average (SA-CASSCF/RASSCF) with equal weights. The subsequent CASPT2 calculations are reported as single-state (SS-) and multistate (MS-CASPT2).[32] The RASPT2 results are only reported in the MS fashion. The number of roots employed in each irreducible representation is specified in the corresponding table caption. Oscillator strengths were calculated at both the SA-CASSCF, MS-CASPT2, and MS-RASPT2 levels of theory through the RAS state interaction method.[33] The core shell orbitals were kept frozen in the CASPT2 calculations in order to avoid BSSE errors. In all our CASPT2/RASPT2 calculations, an ionization potential electron affinity (IPEA) shift (default value of 0.25 au) for the zeroth-order Hamiltonian was employed.[34] Additionally, an extra level shift[35] of 0.3 au was used to prevent weakly coupling intruder states interference, mainly with the high-lying states. Similar values of ca. 0.25 au have been used elsewhere to compute excited states of TM complexes.[9] The spin−orbit (SO) UV−vis spectra have been also computed

**Table 1. Relative SA-CASSCF(14,13) and SS- and MS-CASPT2(14,13) as well as SO-MS-CASPT2(14,13) Electronic Transitions Energies, ΔE (in eV), with Oscillator Strengths *f*, and Main Assignment for Complex 1[a]**

| | SA-CASSCF(14,13)[b] | | | SS-CASPT2 (14,13) | MS-CASPT2(14,13)[c] | | SO-MS-CASPT2(14,13)[c] | |
|---|---|---|---|---|---|---|---|---|
| state | assignment/weight ($c^2$) | *f* | ΔE (eV) | ΔE (eV) | ΔE (eV)/$c^2$ | *f*[d] | ΔE (eV) | *f* |
| $S_0$ ($1^1A_1$) | $^1$GS/0.86 | | | 0.0 | 0.0/0.86 | | 0.0 | |
| $S_1$ ($1^1A_2$) | $^1$MC ($4d_{yz}-a_2\rightarrow 4d_{z^2}-a_1$)/0.71 | 0.000 | 3.15 | 3.76 | 3.76/0.72 | 0.000 (0.000) | 3.78 | 0.000 |
| $S_2$ ($1^1B_1$) | $^1$MC ($4d_{xz}-b_1\rightarrow 4d_{z^2}-a_1$)/0.79 | 0.009 | 3.59 | 3.49 | 3.49/0.77 | 0.009 (0.007) | 3.52 | 0.009 |
| $S_3$ ($2^1B_1$) | $^1$MC ($4d_{yz}-a_2\rightarrow 4d_{x^2-y^2}-b_2$)/0.78 | 0.006 | 4.77 | 4.19 | 4.19/0.76 | 0.004 (0.004) | 4.23 | 0.003 |
| $S_4$ ($2^1A_2$) | $^1$MC ($4d_{xz}-b_1\rightarrow 4d_{x^2-y^2}-b_2$)/0.75 | 0.000 | 4.82 | 4.81 | 4.82/0.77 | 0.000 (0.000) | 4.82 | 0.000 |
| $S_5$ ($2^1A_1$) | $^1$MC ($4d_{xy}-a_1\rightarrow 4d_{z2}$-$a_1$)/0.84 | 0.007 | 5.13 | 5.57 | 5.57/0.85 | 0.006 (0.007) | 5.59 | 0.006 |
| $S_6$ ($1^1B_2$) | $^1$MLCT ($4d_{yz}-a_2\rightarrow \pi^*_{bpy}-2b_1$)/0.76 | 0.000 | 5.19 | 3.81 | 3.73/0.74 | 0.000 (0.000) | 3.74 | 0.000 |
| $S_7$ ($2^1B_2$) | $^1$MC ($4d_{xy}-a_1\rightarrow 4d_{x^2-y^2}-b_2$)/0.82 | 0.001 | 5.32 | 5.49 | 5.55/0.62 | 0.070 (0.018) | 5.57 | 0.068 |
| $S_8$ ($3^1B_2$) | $^1$IL ($\pi_{bpy}-1a_2\rightarrow \pi^*_{bpy}-1b_1$)/0.28 | 0.195 | 5.44 | 5.40 | 5.49/0.30 | 0.049 (-)[e] | 5.51 | 0.051 |
| | $^1$IL ($\pi_{bpy}-1a_2\rightarrow \pi^*_{bpy}-2b_1$)/0.22 | | | | | | | |
| $S_9$ ($3^1A_1$) | $^1$MLCT ($4d_{xz}-b_1\rightarrow \pi^*_{bpy}-2b_1$)/0.85 | 0.045 | 5.61 | 3.35 | 3.35/0.85 | 0.025 (0.059) | 3.36 | 0.025 |
| $S_{10}$($4^1B_2$) | $^1$MLCT ($4d_{yz}-a_2\rightarrow \pi^*_{bpy}-1b_1$)/0.69 | 0.162 | 6.34 | 4.74 | 4.75/0.60 | 0.199 (0.012) | 4.77 | 0.198 |
| $S_{11}$($5^1B_2$) | $^1$IL ($\pi_{bpy}-1a_2\rightarrow \pi^*_{bpy}-2b_1$)/0.52 | 0.405 | 6.64 | 4.65 | 4.49/0.40 | 0.306 (0.309) | 4.50 | 0.306 |

[a] The square of the configuration interaction coefficient, $c^2$, indicates the weight in the wave function of the leading CSF obtained by the indicated electron replacement. [b] SA-(3,3,2,6)-CASSCF(14,13) calculations for $A_1$, $B_1$, $A_2$, and $B_2$ symmetries, respectively. [c] SO-MS/MS-(3,3,2,6)-CASPT2-(14,13) calculations for $A_1$, $B_1$, $A_2$, and $B_2$ symmetries, respectively. [d] In parenthesis, oscillator strengths obtained with MS-RASPT2(16,2,2;3,9,4). [e] This state was not computed at the MS-RASPT2(16,2,2;3,9,4) level of theory.

with the CAS(14,13) wave function. The SO couplings have been evaluated with the SO-RASSI approach[36] (further details can be found in the Supporting Information).

The TD-DFT calculations were performed at the $C_{2v}$ geometry with a 6-311G* basis set (ECP-28-mwb pseudopotential for Ru). The different functionals employed are: (i) several hybrid functionals with an increasing amount of exact exchange in the following order: B3LYP[37] (20% of exact exchange), PBE0[17] (25%), and B3LYP-35[38] (35%); (ii) the meta-hybrid M06[39] and M06-2X[39] functionals (with 27% and 54% of exact exchange, respectively); (iii) the pure functional PBE;[40] and (iv) the long-range corrected CAM-B3LYP and LC-$\omega$PBE functionals. Additionally, TD-DFT calculations were also performed in solution using $CH_3CN$ as solvent with the polarization continuum model,[41] i.e., PCM-TD-DFT calculations, with the same basis set.

The ground-state optimization and TD-DFT calculations have been performed with the Gaussian09[42] program package, while CASSCF/CASPT2 and RASSCF/RASPT2 calculations have been performed with the MOLCAS7.2[43] software.

## 3. RESULTS AND DISCUSSION

First of all, we report here the experimental values known for the complex **1**. The UV−vis spectrum recorded in $CH_3CN$ is characterized by a small band peaking at 352 nm or 3.52 eV (3.62 eV in $CH_2Cl_2$) showing an intensity of 1550 $M^{-1}cm^{-1}$ and by a higher broader band centered at ca. 300 nm or 4.14 eV, with a higher relative intensity of 14 100 $M^{-1}cm^{-1}$.[23,24] The peaks of this main band with their associated intensities are the following: 3.96 eV (14 100 $M^{-1}cm^{-1}$), 4.13 eV (11 300 $M^{-1}cm^{-1}$), and 4.34 (10 000 $M^{-1}cm^{-1}$) Taking these values as a reference, hereafter we shall discuss the values obtained theoretically with the methods described above.

**3.1. CASPT2/CASSCF Calculations.** Table 1 shows the CASPT2/CASSCF(14,13) results for the excited states of complex **1**. The CASSCF(14,13) calculations indicate that the low-lying singlet electronic excitations are mainly weakly absorbing $^1$MC states of different symmetries, see $S_1$−$S_5$ and $S_7$ states at the CASSCF level of theory. We note that among them there are states of $A_2$ symmetry that, although strictly forbidden by symmetry, might be populated, e.g., in the course of photochemical deactivation channels. The $^1$MLCT and $^1$IL states showing substantial oscillator strengths are the $S_8$, $S_9$, $S_{10}$, and $S_{11}$ states at the CASSCF level of theory. The $^1$MLCT states consist of transitions from the 4d orbitals of the Ru atom to the $\pi^*_{bpy}$ orbitals. The $^1$IL states are transitions within the $\pi_{bpy}/\pi^*_{bpy}$ orbitals, and thus excitations retain certain local character. To describe them all simultaneously at the CASSCF level of theory, we need to compute at least six states of $B_2$ symmetry and 3/3/2 states of $A_1/B_1/A_2$ symmetry, respectively. The chosen number of states corresponds to the minimum amount of roots necessary to describe the spectrum below ca. 5 eV in a balance manner, taking into account that some spectroscopic states do not appear as low-energy roots at the CASSCF level of theory and that the final states involved in these transitions have mixed character (see, e.g., $S_8$ and $S_{11}$ in Table 1). Table 1 also contains the SS-CASPT2 and MS-CASPT2 values. Similar energies are obtained with both procedures, being the roots of the $B_2$ irreducible representation the ones most affected by the MS procedure, due to the larger mixing present at the SA-CASSCF level of theory. The inclusion of dynamical correlation via CASPT2 leads to a large stabilization of some $^1$MLCT and $^1$IL states and thus to state reordering. As a consequence, the $S_9$ state ($3^1A_1$) at the CASSCF level of theory, for example, becomes the first excited state with MS-CASPT2 (or SS-CASPT2). On the contrary, dynamical correlation does not severely affect the relative energies of the $^1$MC states, which remain almost unaffected (e.g., $S_2$ and $S_4$) or are slightly blue/red-shifted ($S_1$ and $S_3$, respectively). Returning our attention to the $3^1A_1$ state, this is predicted at 3.35 eV at CASPT2 level of theory and hence in reasonable agreement with the weak band peaking experimentally at ca. 3.52 eV. Note that this state is the lowest at CASPT2 level of theory, while it was the $S_9$ with CASSCF.

Table 2. Selected TD-DFT Electronic Transitions Energies, ΔE (in eV), with Oscillator Strengths *f* against Experimental Values[a]

| | meta-hybrid functionals (% HF exchange) | | | | range-sepatated functionals | | | | hybrid functionals (% HF exchange) | | | | | | pure functionals | | |
|---|---|---|---|---|---|---|---|---|---|---|---|---|---|---|---|---|---|
| | M06 (27%) | | M06-2X (54%) | | CAM-B3LYP | | LC-ωPBE | | B3LYP-35 (35%) | | PBE0 (25%) | | B3LYP (20%) | | PBE | | exptl |
| state | ΔE | *f* | ΔE | *f* | ΔE | *f* | ΔE | *f* | ΔE | *f* | ΔE | *f* | ΔE | *f* | ΔE | *f* | ΔE |
| $1^1B_1$ ($^1$MC) | 2.99 | 0.001 | 3.06 | 0.003 | 3.39 | 0.003 | 3.50 | 0.003 | 3.34 | 0.003 | 3.31 | 0.002 | 3.25 | 0.001 | 3.09 | 0.002 | |
| | *3.00* | *0.002* | *3.02* | *0.003* | *3.38* | *0.004* | *3.46* | *0.004* | *3.33* | *0.004* | *3.34* | *0.004* | *3.30* | *0.003* | *3.19* | *0.003* | |
| $3^1A_1$ ($^1$MLCT) | 2.48 | 0.011 | 3.64 | 0.009 | 3.43 | 0.014 | 4.19 | 0.022 | 3.10 | 0.010 | 2.60 | 0.010 | 2.41 | 0.009 | 1.56 | 0.008 | 3.52[b] |
| | *3.47* | *0.023* | *4.55* | *0.019* | *4.41* | *0.031* | *5.05* | *0.047* | *4.03* | *0.021* | *3.51* | *0.019* | *3.42* | *0.019* | *2.50* | *0.016* | 3.62[c] |
| $5^1B_2$ ($^1$IL) | 4.29 | 0.142 | 4.76 | 0.246 | 4.67 | 0.258 | 4.82 | 0.289 | 4.56 | 0.304 | 4.44 | 0.199 | 4.29 | 0.064 | 4.02 | 0.064 | 3.96[b] |
| | *4.18* | *0.315* | *4.63* | *0.358* | *4.53* | *0.386* | *4.64* | *0.353* | *4.42* | *0.392* | *4.32* | *0.280* | *4.21* | *0.247* | *3.94* | *0.287* | |
| $4^1B_2$ ($^1$MLCT) | 3.35 | 0.002 | 4.66 | 0.067 | 4.51 | 0.016 | 5.65 | 0.014 | 4.08 | 0.001 | 3.49 | 0.002 | 3.25 | 0.001 | 2.19 | 0.002 | 4.13−4.34[b] |
| | *4.42* | *0.071* | *5.77* | *0.022* | *5.71* | *0.034* | *6.68* | *0.139* | *5.01* | *0.029* | *4.49* | *0.107* | *4.36* | *0.123* | *3.21* | *0.002* | |

[a] Numbers in italics are calculated in solution ($CH_3CN$) with the PCM model. [b] In $CH_3CN$, from ref 23. [c] In $CH_2Cl_2$, from ref 24.

This demonstrates the importance of dynamical correlation on the different type of states, as explained above. For simplicity, and although the order of states is altered in many cases with the addition of the PT2 correction, in the following discussion we keep the state numbers as provided by the CASSCF method. In view of the high oscillator strengths obtained with CASSCF for the $S_{11}$ ($5^1B_2$) and $S_{10}$ ($4^1B_2$) states, theoretically predicted at 4.49 and 4.75 eV at the MS-CASPT2 level of theory, these states can be then considered responsible of the strong band peaking at 3.96 and 4.13−4.34 eV. These states are ca. 0.5 eV blue shifted with respect to the experiment, but one should keep in mind that the experimental data are obtained in the presence of solvent, not included in the present calculations.

Regarding the intensities of the calculated states, as it can be seen in Table 1, all the $^1$MC states as well as the $S_6$ ($^1$MLCT) state are almost dark at both the CASSCF and CASPT2 levels of theory. The intensities of the bright $S_{11}$ and $S_{10}$ states are consistent at both the CASSCF and CASPT2 levels of theory. Accordingly, the oscillator strength of the $^1$IL ($S_{11}$) state is higher than the one of the $^1$MLCT ($4^1B_2$) state. This is in agreement with the experimental evidence, since higher intensities are obtained for the band at 3.96 than for the one peaking at ca. 4.13−4.34 eV.

The previous analysis serves to focus on some relevant states (the $4^1B_2$ and $3^1A_1$ MLCT states, the $5^1B_2$ IL state, and exemplarily one MC state ($1^1B_1$)) for which the CASPT2/CASSCF results will be compared with different TD-DFT and RASPT2/RASSCF protocols in the coming subsections. However, before proceeding to discuss such calculations, we have considered of interest to analyze the SO effects on the spectroscopic properties of complex **1**. The SO-MS-CASPT2(14,13) values are also tabulated in Table 1 and illustrate that energetic shifts are present in all the low-lying excited states of complex **1**. The biggest shift is found in the case of the $2^1B_1$ state ($^1$MC state), amounting up to 0.04 eV as compared to the spin-free MS-CASPT2(14,13) value. The resulting SO state is mixed with a close-lying triplet excited state (the spin-free contributions of the resultant SO state are 72% of $2^1B_1$ and 25% of $2^3A_2$; the lowest lying triplet excited states are summarized in Table S1 of the Supporting Information). Such strong mixing is expected in states with participation of the ruthenium center, such as the $^1$MC states. The SO shifts obtained here are comparable to those obtained in other TM complexes, e.g., Os complexes.[44] In summary, the SO effects modify the spectroscopic properties of complex **1** but not significantly. SO effects are on the other hand indispensable to the interpretation of many other photophysical phenomena, such as intersystem crossing (ISC) rates. We note that very large SO couplings (ca. 280 $cm^{-1}$) are found between the $3^1A_1$ and $T_1$ ($1^3A_2$) states, which lie almost degenerate in energy favoring the ISC.

**3.2. TD-DFT Calculations.** The results obtained with different functionals for the excited states specified above are collected in Table 2. The values including $CH_3CN$ are given in italics. The $^1$MC state ($1^1B_1$ state, following the CASSCF label of Table 1) is predicted within all the employed functionals in a range of ca. 0.4 eV, being rather immune to solvent effects. It has been previously seen that TD-DFT can succeed to describe d−d transitions of closed-shell TM carbonyl complexes,[45] such as $Cr(CO)_6$.[46] On the other hand, as pointed by Neese and co-workers, TD-DFT has drawbacks when describing d−d transitions in problematic configurations like $d^5$ situations; for example, errors exceeding 0.6 eV were found in the TD-DFT energies of the $[Ni(H_2O)_6]^{2+}$ complex ($d^8$ configuration) with the B3LYP functional.[16] TD-B3LYP was even not capable to reproduce the correct number of d−d excitations in this complex because some of them contained substantial double excitation character that TD-DFT cannot handle within the constraint of the adiabatic approximation. In our closed-shell complex **1**, meta-hybrids (namely the M06 and M06-2X) tend to slightly underestimate the d−d transition energy, especially M06, which yields the highest deviation (ca. 0.3−0.4 eV) in comparison to the rest of TD-DFT values and the MS-CASPT2(14,13) results. The range-separated functionals yield the larger values for the $^1$MC state, especially the LC-ωPBE functional which predicts 3.50 eV in good agreement with the CASPT2 value. Both hybrid and pure functionals predict the energy of the $1^1B_1$ state in a small range. We note that the larger the percentage of exact HF-exchange is contained in the hybrid functionals, the higher are the excitation energies corresponding to the d−d transition; thus, B3LYP-35 (35% of exact exchange), PBE0 (25%), and B3LYP (20%) yield values of 3.34, 3.31, and 3.25 eV, in the gas phase, respectively. From all these values, we conclude that overall a reasonable description of the $^1$MC states

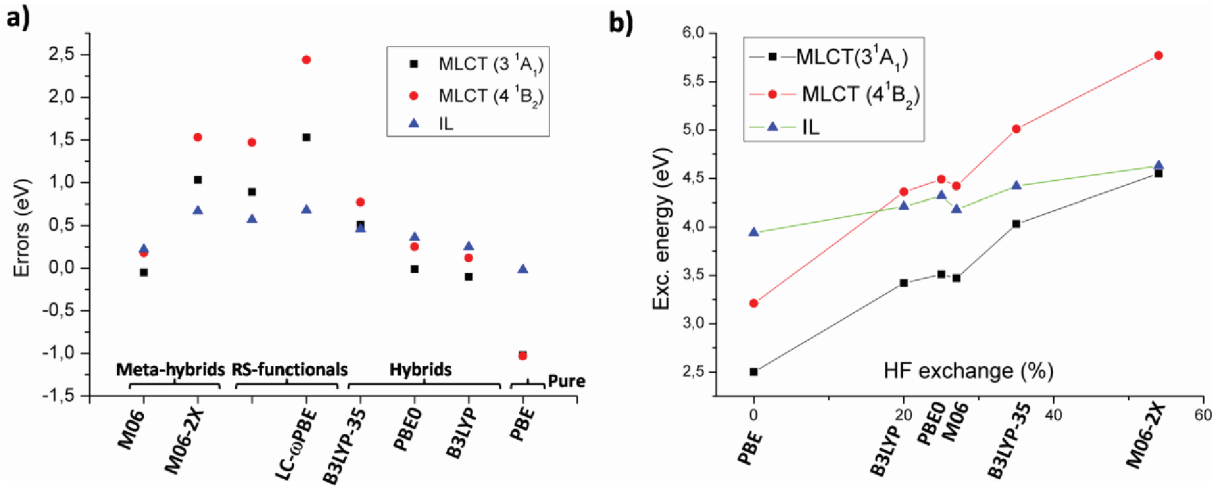


**Figure 3.** (a) PCM-TD-DFT errors (eV) in the electronic excitation energies of complex **1** for different types of excited states. (b) PCM-TD-DFT vertical excitation energies versus percentage of HF exchange of the density functionals for different types of excited states.

can be obtained for complex **1** with TD-DFT, and therefore we expect a similar success for $^1$MC states in other related closed-shell Ru(II) polypyridyl complexes.

Regarding the $^1$MLCT states of complex **1**, namely the $3^1A_1$ and $4^1B_2$ states, one can clearly see at first sight the failure of some functionals behavior, which is well-known in CT states of organic dyes.[47] These states are specially subject of changing in the presence of a polar solvent. Indeed, both $^1$MLCT states are blue shifted by ca. 1 eV as compared to the gas phase values. It is worth noting that this effect manifests regardless the employed functional. Therefore, only the PCM-TD-DFT data will be compared with the experiment. The pure PBE functional leads to underestimations exceeding 1 eV for both $^1$MLCT states. An adequate description of $^1$MLCT states relies heavily on the choice of the functional. Conventional hybrid functionals have a clear tendency to increase the excitation energy of the $^1$MLCT states with increasing exact exchange. For instance, we see that the $3^1A_1$ state is predicted at 3.42, 3.51, and 4.03 eV with B3LYP, PBE0, and B3LYP-35, respectively. These excitation energies are in good agreement with the experimental evidence, especially the B3LYP and PBE0 values. The best result for the $^1$MLCT states is obtained with the functional bearing an intermediate amount of exact exchange, i.e., PBE0, which delivers a deviation from the experiment of only 0.01 eV for the $3^1A_1$ state. Indeed, $^1$MLCT states have been found to be best described with this functional for similar Ru complexes.[48] The trend of larger errors with increasing amount of exact exchange is also observed in the meta-hybrid functional M06 and M06-2X. The $3^1A_1$ state is best described with the M06 functional (27% of exact exchange) which delivers a value of 3.47 eV (error 0.05 eV). The recently developed range-separated functionals employed here perform differently for describing the $^1$MLCT states of complex **1**. LC-$\omega$PBE hugely overestimates the excitation energies of the $^1$MLCT states (e.g., the $4^1B_2$ state is overestimated by more than 2 eV). Interestingly, we note that CAM-B3LYP performs worse than the hybrid functionals B3LYP-35, PBE0, B3LYP, and M06. The $3^1A_1$ state is theoretically predicted at 4.41 eV, and hence the error with respect to the experiment amounts almost to 1 eV. The $4^1B_2$ state is also overerestimated by 1 eV (see Table 2). This evidence is contrary to the good performance of CAM-B3LYP in the treatment of CT states of organic dyes.[49] But indeed, the agreement of CAM-B3LYP to describe MLCT states of other TM complexes[21d,50] is not better. In any case, it is fair noting that the errors coming from different sources, as e.g., the selection of the exchange−correlation functional or the solvation method, might cancel among them leading to inconclusive results. We are confident, nevertheless, that the PCM method, despite its limitations, performs well in this complex.

The energies of the $^1$IL state are not as strongly dependent on the functional as the $^1$MLCT states, yielding values in the gas phase for the $3^1B_2$ state that range from 4.82 eV with the LC-$\omega$PBE functional to 4.02 eV with the pure PBE functional. We note that, oppositely to the $^1$MLCT states, inclusion of solvent effects within the limits of the PCM model leads only to red shifts of ca. 0.1 eV (in all the functionals, see Table 2). Among the hybrid functionals, the excitation energies are lower the smaller the amount of HF exchange, as it happened with the $^1$MC and $^1$MLCT states. Interestingly, and in concordance with the $^1$MLCT states, the agreement with the experiment is obtained with PBE, B3LYP, M06, or PBE0 (with errors for all the functionals well below 0.30 eV), rather than with functionals containing high percentage of exact exchange (as B3LYP-35 or M06-2X) or the range-separated functional CAM-B3LYP, even though the errors for the latter functional are in the acceptable range of accuracy of TD-DFT (ca. 0.57 eV). A similar behavior has been also observed for conjugated organic compounds, where the small maximum average errors in the description of local $\pi\pi^*$ excitations are obtained with the PBE0 functional.[20]

Since the PCM-TD-DFT values look trustworthy, as long as a proper functional is chosen, we assign the UV−vis spectra of complex **1** in the following way: The weak band peaking at ca. 3.52 eV is due to the $3^1A_1$ $^1$MLCT state. The strong band peaking at 3.96 and 4.13−4.34 eV, with absorption intensities of 14 100 and 11 300−10 000 $M^{-1}cm^{-1}$, respectively, can be attributed to the $5^1B_2$ ($^1$IL) and the $4^1B_2$ ($^1$MLCT) states, respectively. Such assignment is done in view of the energetic order the last two states, which is reproduced with most of the TD-DFT flavors (in the presence of solvent) and the MS-CASPT2(14,13) calculations. The oscillator strengths of both states are also in accordance to this assignment. Thus, the $^1$IL state possesses higher oscillator strength than the $^1$MLCT state, in accordance to the experimental absorption intensities.

**Table 3. Relative RASSCF($n,l,m;i,j,k$) and RASPT2($n,l,m;i,j,k$) Electronic Transitions Energies, $\Delta E$ (in eV), of the Main Electronic Excitations of Complex 1, at Different Levels of Theory, Compared to the SA-CASSCF and MS-CASPT2 and Available Experimental Data**

| States | SA-CAS (14,13) | MS-CASPT2 (14,13) | SA-RAS (16,4,4; 8,0,8)[a] | MS-RASPT2 (16,4,4; 8,0,8)[b] | SA-RAS[a] (16,$l,m$; 2,11,3) | | | MS-RASPT2[b] (16,$l,m$; 2,11,3) | | | SA-RAS (16,2,2; 3,9,4)[a] | MS-RASPT2 (16,2,2; 3,9,4)[b] | SA-RAS (22,2,2; 6,9,6)[a] | MS-RASPT2 (22,2,2; 6,9,6)[b] | SA-RAS (16,3,3; 4,7,4)[c] | MS-RASPT2 (16,3,3; 4,7,4)[d] | Exptl |
|---|---|---|---|---|---|---|---|---|---|---|---|---|---|---|---|---|---|
| | | | | | $l,m$ =2 | $l,m$ =3 | $l$=3, $m$=4 | $l,m$ =2 | $l,m$ =3 | $l$=3, $m$=4 | | | | | | | |
| $1\,^1B_1$ ($^1$MC) | 3.59 | 3.49 | 4.50 | 3.36 | 3.99 | 4.03 | 4.04 | 3.31 | 3.31 | 3.31 | 4.20 | 3.23 | 4.53 | 3.55 | 5.10 | 3.36 | - |
| $3\,^1A_1$ ($^1$MLCT) | 5.61 | 3.35 | 5.70 | 4.32 | 5.18 | 5.22 | 5.22 | 3.36 | 3.35 | 3.35 | 5.51 | 3.92 | 5.33 | 3.83 | 4.11 | 3.34 | 3.52[e] 3.62[f] |
| $5\,^1B_2$ ($^1$IL) | 6.64 | 4.49 | 6.41 | 4.83 | 6.08 | 6.07 | 6.07 | 4.83 | 4.85 | 4.87 | 6.83 | 4.19 | 6.62 | 4.30[g] | 7.07 | 3.70 | 3.96[e] |
| $4\,^1B_2$ ($^1$MLCT) | 6.34 | 4.75 | 6.92 | 4.57 | 6.58 | 6.57 | 6.58 | 4.58 | 4.61 | 4.62 | 6.35 | 3.96 | 6.17 | 4.61[g] | 6.07 | 3.96 | 4.13[e] |
| Number of CSF's | 183150 | | 73108 | | 2230837($l,m$=2); 5495197 ($l,m$=3); 7399206 ($l$=3, $m$=4) | | | | | | 557036 | | 3890064 | | 390737 | | |

[a] SA-(3,3,4)-RASSCF($n,l,m;i,j,k$) calculations for $A_1$, $B_1$, and $B_2$ symmetries, respectively. [b] MS-(3,3,4)-RASPT2($n,l,m;i,j,k$) calculations for $A_1$, $B_1$, and $B_2$ symmetries, respectively. [c] SA-(3,3,5)-RASSCF($n,l,m;i,j,k$) calculations for $A_1$, $B_1$, and $B_2$ symmetries, respectively. [d] MS-(3,3,5)-RASPT2($n,l,m;i,j,k$) calculations for $A_1$, $B_1$, and $B_2$ symmetries, respectively. [e] In $CH_3CN$, from ref 23. [f] In $CH_2Cl_2$, from ref 24. [g] These states are strongly mixed at the MS(4)-RASPT2(22,2,2;6,9,6) level of theory.

A comment on the performance of the different TD-DFT flavors to predict oscillator strengths is in order here. As expected and in agreement with the experiment, the intensity of the $^1$MC state is very low, no matter which functional is used or whether solvation is included. Noteworthy, the oscillator strengths of the $^1$MLCT states computed in the gas phase are underestimated with all the functionals in comparison to the PCM-TD-DFT values; very likely, this error is connected to the underestimation of the excitation energies, among other effects. The least robust excitation is the one corresponding to the intense $^1$IL state, whose results are dependent on the functional employed. In gas phase, PBE and B3LYP predict oscillator strengths thrice smaller than the rest of functionals. The reason behind this fact might be the mixing of the intense $^1$IL state with an n$\pi^*$ excitation, as reflected on the wave function coefficients. See, for example, that the $\pi\pi^*$/n$\pi^*$ excitation wave function coefficients in the $^1$IL state with the B3LYP functional are 0.52/0.46, respectively, while with the PBE0 functional, such values are 0.65/0.20, respectively. A more uniform picture is obtained by comparing the PCM-TD-DFT oscillator strengths since all the functionals predict similar values for the $^1$IL state.

In summary it can be seen that the different functionals examined here show a different performance on the calculations of the low-lying excited states of complex **1**. Figure 3a displays the errors in the energy of the PCM-TD-DFT values of the $^1$IL and the $^1$MLCT states, taking as a reference the experimental values. A direct comparison between the oscillator strengths and the absorption intensities is not possible since some of the experimental bands overlap. Additionally, Figure 3b shows the excitation energies for relevant $^1$MLCT and $^1$IL states as a function of the percentage of HF exchange of the employed pure and hybrid/meta-hybrid functionals. There it can be clearly seen that higher energies are obtained with higher percentages of HF exchange, being the effect more pronounced for the MLCT states. Similar trends have been observed for other Ru complexes.[48] As discussed before, acute problems are found in the description of $^1$MLCT states. These are only accurately calculated by hybrid functionals with intermediate percentages of exact exchange; the functionals M06, PBE0, and B3LYP, in this order, give the best accuracy when solvent effects are considered. These three functionals plus the pure functional PBE seem to be the only ones which are able to get a reasonable value of the local $^1$IL excitation of **1**. Based on these results, the best balanced description of all kind of excited states of Ru(II)−polypyridyl complexes can be best obtained with M06 in first place and B3LYP and PBE0 in second and third places, respectively, even though slight underestimations of the d−d transition are found for the M06 functionals. The inclusion of solvent effects is mandatory, especially for the $^1$MLCT states. Indeed, this combination (an hybrid functional with intermediate amount of exact exchange and the consideration of solvent effects via the PCM method) has been successfully used in other Ru(II) polypyridyl complexes.[21b,c] In this sense, it is surprising that the CAM-B3LYP functional, designed a priori to deal with CT states does not improve the conventional hybrid functionals when describing both the $^1$MLCT and $^1$IL states. Very likely, the bad performance of CAM-B3LYP for describing $^1$MLCT states is due to the short distance between the donor and acceptor moieties. In contrast to these conclusions, the pure PBE functional (also in combination with solvent effects) has been found to outperform the B3LYP functional in the description of the excited states of $Fe(phen)_2(CN)_2$.[51] The reason behind the good performance of the pure functional PBE in this particular situation is probably the mixing of the d-based orbitals with the ligand-based orbitals, leading to an overlap of the orbitals involved in the state and hence to a loose CT character of these states. Another possible explanation might be cancellation effects, as we stated above. Whether this situation takes place in others TM complexes needs to be evaluated for each particular case.

**3.3. RASPT2/RASSCF Calculations.** The energies and oscillator strengths obtained with the different RASPT2/RASSCF protocols are compiled in Table 3. The computational strategies that we will discuss below have been chosen following two intentions: The first is to improve the quality of the previous CASPT2/CASSCF using an affordable configuration space. The second is to find general hints about how to face the treatment of excited states of related TM complexes at the RASPT2/RASSCF level of theory.

As a first step with respect the CAS(14,13) calculations, we include the $n_{Cl}-a_1$ orbital and two $\pi^*_{CO}$ orbitals ($\pi^*_{CO}-b_1$ and


dx.doi.org/10.1021/ct200640q | J. Chem. Theory Comput. 2012, 8, 203–213

$\pi^*_{CO}-a_2$) in the active space. The simplest approach is to distribute all the orbitals within RAS1 and RAS3 subspaces and leave the RAS2 empty while allowing SDTQ excitations within the RAS1/RAS3 subspaces. This is denoted as RASSCF(16,4,4;8,0,8). As it can be seen in Table 3, the number of CSFs is heavily reduced in comparison to the CASSCF(14,13) calculations, by almost a factor of 3. Unfortunately, while cheap and easy, this procedure leads to poor results for both the low- and high-lying excited states. The $3^1A_1$ state, calculated at 3.35 eV with CASPT2(14,13), is now predicted at 4.32 eV with RASPT2(16,4,4;8,0,8) and hence deviating 1 eV from the CASPT2 value. The RASPT2(16,4,4;8,0,8) relative energies of the high-lying $5^1B_2$ and $4^1B_2$ bright states are only about 0.3−0.2 eV different from the CASPT2(14,13) values but with shifts in different directions. An important difference between both methodologies is that, as a consequence of this reverse shift, the $^1$MLCT ($4^1B_2$) state is below the $^1$IL state ($5^1B_2$) at the RASPT2(16,4,4;8,0,8) level of theory. The latter result is suspicious in view of the previous CASPT2 and TD-DFT results. In principle, the solvent effects could reverse the order of the states, since the $^1$MLCT state is more sensible than the $^1$IL state to solvatochromic effects, as reflected with the PCM-TD-DFT calculations. Unfortunately, RASPT2 calculations in the presence of solvent effects are difficult and computationally too demanding to be investigated, so that no further conclusions can be reached. We note however that leaving the RAS2 empty has also given poor results in describing the singlet−triplet splitting of copper complexes.[12] Even though this strategy had resulted useful in describing ionization and low-lying excited states of simple systems, such as organic $\pi$ conjugated compounds,[10] the results obtained in this work also seem to confirm that in TM complexes better results are obtained if the RAS2 subspace is not empty.

Therefore, in the following we focus on finding the optimal composition of the RAS2 subspace, which, as we will show, is indeed the crucial step to obtain a balanced and accurate description of the relevant excited states of **1**. Moving the $n_{Cl}-a_1$, the $\pi_{bpy}-2a_2/\pi^*_{bpy}-2a_2$ pair and the two $\pi^*_{CO}$ orbitals to the RAS1/RAS3 subspaces leads to the RASSCF(16,*l*,*m*;2,11,3) calculations, which will allow up to D, T, or Q excitations, depending on the *l* and *m* indexes. As we see in Table 3, the introduction of these orbitals and therefore further correlation in the zeroth-order wave function implies a slightly better description of some states. Exemplarily, the $3^1A_1$ states goes from 5.61 eV at CASSCF(14,13) to 5.18 eV at RASSCF(16,2,2;2,11,3) level. The perturbative treatment leads to very similar results: the $3^1A_1$ state is predicted at 3.36 eV with RASPT2(16,2,2;2,11,3) level of theory, and the $5^1B_2$ and $4^1B_2$ states are now located at 4.83 and 4.58 eV, respectively. The results seem to be hardly improved with respect to the CASPT2(14,13) results, since the transition responsible for the lowest energy band is located at the same position and the error with respect to the peaks higher in energy ($5^1B_2$ and $4^1B_2$) is now ca. 0.9 and 0.4 eV, respectively (obviating several effects, e.g., solvatochromic effects) at the RASPT2(16,2,2;2,11,3) level of theory. An improvement of these results can be attempted following two strategies: either increasing the allowed excitations within the RAS1/3 subspaces or changing the current RAS partition.

First, we shall discuss the former strategy. Allowing up to triple excitations is labeled by RASSCF(16,3,3;2,11,3), while up to triples−quadruples (*l* = 3 and *m* = 4) is denoted by RASSCF(16,3,4;2,11,3). As it can be seen, the number of CSFs for such approaches is over 5 and 7 million, respectively, on the limit of computational feasibility. Disappointingly, as it can be seen in Table 3, the relative energies of all the states show negligible changes regardless the level of excitation, at both RASSCF and RASPT2 levels of theory. These calculations do highlight that an enormous number of CSFs does not guarantee the quality of the results. If the orbitals composing RAS2 subpace are not properly selected to achieve a reasonable reference space, then perturbation theory will not be able to get accurate results.

Therefore, we turn our attention to redefine the RAS partition. An additional pair of $\pi_{bpy}/\pi^*_{bpy}$ orbitals ($\pi_{bpy}-1b_1/\pi^*_{bpy}-1a_2$) with high and low occupation numbers, respectively, is moved from the RAS2 to the RAS1/3 subspaces. This strategy has the additional advantage that, in principle, it allows to include additional orbitals in the RAS1/3 subspaces because now the number of CSFs is considerably reduced. Allowing SD excitations is labeled as RASSCF(16,2,2;3,9,4) calculations. As it can be seen in Table 3, the number of CSF's is reduced by a factor of 10 in comparison to the RASSCF(16,2,2;2,11,3) calculations. Very interestingly, we note that the results obtained with the economic RASPT2(16,2,2;3,9,4) level of theory seem to be more balanced than the previous ones. The low-lying $3^1A_1$ state is now predicted at 3.92 eV. If we consider the solvatochromic blue shift calculated with the PCM-TD-DFT model, this state deviates even more from the experiment than the previous RASPT2 schemes. On the other hand, we believe that the $5^1B_2$ and $4^1B_2$ states, located now at 4.19 and 3.96 eV, are in closer agreement with the experimental evidence. Thus, the $^1$IL state is only accurately described within this latter procedure (recall that solvatochromic effects are not so important for this state, as reflected by the PCM-TD-DFT calculations). Additionally, the $4^1B_2$ $^1$MLCT state is also better predicted at this level of theory in comparison to the previous RASPT2 results, assuming also a solvatochromic blue shift. The $^1$MC ($1^1B_1$) state seems to be rather immune to electronic correlation, and it is located at 3.23 eV, a very similar value as that obtained with the other RAS calculations. We note that the maximum deviations in the case of the $^1$MC state, among the different RASPT2 calculations, amount only to ca. 0.3 eV. This is due to the immunity of these states to static correlation effects. Indeed, deviations in the same order of eV have been reported analogously for different CASPT2 calculations in other TM complexes.[30] The RASPT2(16,2,2;3,9,4) oscillator strengths at this level of theory are reported in parenthesis in Table 1. In most of the cases, the oscillator strengths are in agreement with the MS-CASPT2(14,13) ones. The main discrepancy is found in the $S_{10}$ ($4^1B_2$) state, where RASPT2(16,2,2;3,9,4) predicts more than 1 order of magnitude smaller oscillator strength. Since the gas phase TD-DFT results also point to a weak $4^1B_2$ state, we are confident that the RASPT2(16,2,2;3,9,4) oscillator strengths are trustable.

Inclusion of further correlation orbitals leads to the RASPT2/RASSCF(22,2,2;6,9,6) calculations. With a few million of CSF's, these calculations are on the computational limit and would be prohibitive at the CASPT2/CASSCF level of theory. They are probably an illustration of the size of TM−polypyridyl complexes that can be nowadays calculated at the RASPT2/RASSCF level of theory. Moreover, and more interestingly, they allow evaluating whether all the correlation orbitals are necessary to get accurate results for complex **1**. As it can be seen in Table 3, the low-lying $3^1A_1$ state is slightly better described than at the RASPT2(16,2,2;3,9,4) level of theory. The $^1$IL state is also

accurately predicted at the RASPT2(22,2,2;6,9,6) level of theory, and the $^1$MC ($1^1B_1$) state seems to be (again) unaffected by the inclusion of further correlation effects. On the other hand, the $^1$MLCT ($4\ ^1B_2$) state is blue shifted as compared to the RASPT2(16,2,2;3,9,4) calculations, exhibiting similar values to the rest of CASPT2 and RASPT2 values. We note however that at this level of theory, the intense $^1$IL ($5^1B_2$) and the $^1$MLCT ($4^1B_2$) states are strongly mixed. For example, the wave function coefficients of the configuration state function obtained by the $4d_{yz}-a_2\rightarrow\pi^*_{bpy}-1b_1/\pi_{bpy}-1a_2\rightarrow\pi^*_{bpy}-2b_1$ excitations are 0.38/0.38, in the case of the latter state. As a consequence of this mixing (which we consider unlikely as compared to the rest of CASPT2 and RASPT2 calculations performed), the oscillator strengths computed at the alternative RASPT2(16,2,2;3,9,4) level of theory can be considered more accurate. Probably, a higher number of average states is necessary to describe correctly the $B_2$ states with this active space, but due to the expensive cost of these calculations, no further trials have been done. Therefore, when going from the RASPT2(16,2,2;3,9,4) to the RASPT2(22,2,2;6,9,6) calculations, almost no improvement in the relative energies is achieved. The more economic RASPT2-(16,2,2;3,9,4) partition is more valuable here, giving intensities in closer agreement with the experiment and the PCM-TD-DFT values.

In view of the rather poor improvement when going from the RASPT2(16,2,2;3,9,4) to the RASPT2(22,2,2;6,9,6) calculations, we have again reformulated the partition of the RAS subspaces so that $\sigma-\pi$ correlation is primary described with the RAS2. In the RASPT2/RASSCF(16,3,3;4,7,4) calculations, the RAS2 subspace is then composed by the correlation orbitals, and SDT excitations are allowed within the RAS1/3 orbitals. Noteworthy, such calculations are more economic than the RASSCF(16,2,2;3,9,4) ones, being the number of CSF's only twice that of the ones spanned by a (14,13) active space. As it can be seen in Table 3, the RASPT2 (16,3,3;4,7,4) results are the most accurate. The $^1$IL and $^1$MC are accurately described in comparison to the experiment and the TD-DFT calculations (recall that these states are rather immune to solvent effects at the PCM-TD-DFT level of theory). The $^1$MLCT states are now predicted at 3.34 ($3^1A_1$) and 3.96 ($4^1B_2$) eV, yielding the closest results to the experiment among all the RASPT2 calculations even after the expected blue shift due to the solvent.

Summarizing, it seems that the main bottleneck to obtain a balanced description of the excited states of Ru(II) polypyridyl complexes is the RAS2 partition. Our RASPT2 (16,3,3;4,7,4) results indicate that to get spectroscopic accuracy, the correlation orbitals should be included into the RAS2, while those orbitals participating into the main excitations should be included into the RAS1/3. In contrast to these conclusions, Sauri and co-workers have reported that for the excited states of a free-base porphin, the highest accuracy is obtained when the MOs involved in the main excitations are included in the RAS2 subspace.[11] This advice can also be followed in TM complexes, as long as it is computationally feasible. In cases where this is not the case (which unfortunately can be many), our computations conclusively demonstrate that correlation orbitals involved in covalent metal−ligand bonds should be the ones first included into the RAS2. In the title molecule, this strategy, leading to the partition RASPT2 (16,3,3;4,7,4), also pays off in comparison with CASPT2(14,13), especially in the calculation of high-lying excited states, such as the $4^1B_2$ state. There is an evident improvement in the description of the latter state achieved due to the proper treatment of the very important static correlation effects related to covalent metal−ligand bonds; and most importantly, at almost no further computational expense. We truly believe that these strategies will open the study of other larger 4d, and even 5d, TM complexes with strong covalent metal−ligand bonds using the RASPT2 method. In complexes, such as $[Ru(bpy)_3]^{2+}$, many MLCT, IL, and ligand-to-ligand CT transitions are found in the low-energy region as a consequence of the many low-lying $\pi/\pi^*$ orbitals located on the ligands. Following our recipe, these ligand orbitals could be better allocated into the RAS1/3, leaving the RAS2 free for relevant correlation orbitals involved in covalent metal−ligand bonds. Only in this way these complexes, otherwise unreachable for CASPT2, might be faced with RASPT2.

## 4. CONCLUDING REMARKS

TM complexes are prototypes of systems where transitions of very different character, i.e., IL, MC, MLCT, and LMCT states, can be found. This makes them specially complicated to handle computationally so that balanced results can be obtained for all the excited states simultaneously. As an example of such a situation, we have calculated the excited states of the *trans*-(Cl)-Ru(bpy)$Cl_2(CO)_2$ complex with CASPT2/CASSCF and RASPT2/RASSCF protocols, allowing different partitions of the active space and different excitation levels. As found in the case of some organic and inorganic systems,[11] in order to get accurate results, the inclusion of correlation orbitals in the active space is important, however, much more significant seems to be the choice of the partition of the RAS subspaces, especially the RAS2. From the results obtained here, we conclude that at least for this type of Ru complexes, the RAS2 subspace should not be empty, but it must contain the correlation orbitals involved in the covalency of the metal−ligand bonds and only those. The orbitals involved in the main electronic excitations should be better allocated to the RAS1 and RAS3 subspaces. Once an optimal partition is achieved, SDT excitations within the RAS1/3 subspaces are sufficient to handle the additional dynamical correlation and thus obtain the right order of the states with accurate energies and intensities. These hints should be transferable to compute excited states of analogue complexes with strong covalent metal−ligand bonds, like the $[Ru(bpy)_3]^{2+}$ complex, at the RASPT2/RASSCF level of theory. Needless to say, additional molecules should be studied before universal trends can be drawn.

The performance of several TD-DFT flavors is herein also assessed. Desirable is a general method which allows describing the different transitions contributing to the UV−vis spectrum. Solvent effects are found to be mandatory to obtain spectroscopic accuracy, especially in the case of MLCT states. We find that while MC transitions are rather robust to any of the functionals tested, MLCT states are only well described with functionals bearing intermediate amounts of exact exchange, such as M06, PBE0, and B3LYP, in combination with solvent effects. IL states are also best described with these functionals. In view of these conclusions, here we find that the best compromise to treat all the excited states of Ru(II)−polypyridyl complexes in a balanced manner is first M06, and then the B3LYP and PBE0 functionals. Further benchmark studies are required to establish general trends in TM spectroscopy.

This study clearly shows that the rationalization of the UV−vis spectra of TM complexes exclusively based on the matching of

experimental and theoretical TD-DFT bands might be dangerous without an initial exploration of the performance of different hybrid or range-separated functionals because some $^1$MLCT states might be theoretically underestimated (by more than 1 eV in some cases) but match accidentally a different band of the experimental spectrum.

## ■ ASSOCIATED CONTENT

**Supporting Information.** The relative SA-CASSCF-(14,13) and MS-CASPT2(14,13) lowest lying triplet excited states are shown in Table S1. This material is available free of charge via the Internet at http://pubs.acs.org.

## ■ AUTHOR INFORMATION


### Corresponding Author

*E-mail: leticia.gonzalez@univie.ac.at

### Present Addresses

†Max-Planck-Institut für Kohlenforschung. Kaiser-Wilhelm-Platz 1, 45470 Mülheim an der Ruhr, Germany.

‡Institute for Theoretical Chemistry, University of Vienna, Währingerstrasse 17, 1190 Vienna, Austria.


### Notes

The authors declare no competing financial interest.

## ■ ACKNOWLEDGMENT

This work has been funded by the Carl-Zeiss foundation (D.E.). Computer time in the Rechnenzentrum of the Friedrich-Schiller-Universität Jena is gratefully acknowledged. We are grateful to S. Vancoillie for fruitful discussions and one of the referees for pointing to the solvatochromic shifts, which turned to be rather crucial to interpret the spectrum of *trans*(Cl)-Ru(bpy)$Cl_2(CO)_2$.

## ■ REFERENCES


(1) (a) Gust, D.; Moore, T. A.; Moore, A. L. *Acc. Chem. Res.* **2009**, *42*, 1890–1898. (b) Rau, S.; Schäfer, B.; Gleich, D.; Anders, E.; Rudolph, M.; Friedrich, M.; Görls, H.; Henry, W.; Vos., J. G. *Angew. Chem., Int. Ed.* **2006**, *45*, 6215–6218. (c) Tschierlei, S.; Karnahl, M.; Presselt, M.; Dietzek, B.; Guthmuller, J.; González, L.; Schmitt, M.; Rau, S.; Popp., J. *Angew. Chem., Int. Ed.* **2010**, *122*, 4073–4076.

(2) (a) Concepcion, J. J.; Jurss, J. W.; Brennaman, M. K.; Hoertz, P. G.; Patrocinio, A. O. T.; Iha, N. Y. M.; Templeton, J. L.; Meyer, T. J. *Acc. Chem. Res.* **2009**, *42*, 1945–1955. (b) Romain, S.; Vigara, L.; Llobet, A. *Acc. Chem. Res.* **2009**, *42*, 1944–1953.

(3) (a) O'Regan, B.; Grätzel, M. *Nature* **1991**, *353*, 737. (b) Hagfeldt, A.; Grätzel, M. *Acc. Chem. Res.* **2000**, *33*, 269. (c) Grätzel, M. *Nature* **2001**, *414*, 338. (d) Grätzel, M. *Pure Appl. Chem.* **2001**, *73*, 459. (e) Benkö, G.; Kallioinen, J.; Korppi-Tommola, J. E. Y.; Yartsev, A. P.; Sundström, V. *J. Am. Chem. Soc.* **2002**, *124*, 489–493. (f) Kallioinen, J.; Benkö, G.; Myllyperkiö, P.; Khriachtchev, L.; Skårman, B.; Wallenberg, R.; Tuomikoski, M.; Korppi-Tommola, J.; Sundström, V.; Yartsev, A. P. *J. Phys. Chem. B* **2004**, *108*, 6365–6373. (g) Grätzel, M. *Inorg. Chem.* **2005**, *44*, 6841.

(4) Andersson, K.; Malmqvist, P.-A.; Roos, B. O. *J. Chem. Phys.* **1992**, *96*, 1218.

(5) González, L.; Escudero, D.; Serrano-Andrés, L. *Chem. Phys. Chem.* **2011**, DOI: 10.1002/cphc.201100200.

(6) Pierloot, K.; Vancoillie, S. *J. Chem. Phys.* **2006**, *125*, 124303.

(7) Gindensperger, E.; Köppel, H.; Daniel, C. *Chem. Comm.* **2010**, *46*, 8225–8227.

(8) (a) Olsen, J.; Roos, B. O.; Jorgensen, P.; Jensen, H. J. A. *J. Chem. Phys.* **1988**, *89*, 2185. (b) Malmqvist, P.-A.; Rendell, A.; Roos, B. O. *J. Chem. Phys.* **1990**, *94*, 5477.

(9) Malmqvist, P. −Å.; Pierloot, K.; Shahi, A. R. M.; Cramer, J. C.; Gagliardi, L. *J. Chem. Phys.* **2008**, *128*, 204109.

(10) Shahi, A. R. M.; Cramer, C. J.; Gagliardi, L. *Phys. Chem. Chem. Phys.* **2009**, *11*, 10964–10972.

(11) Sauri, V.; Serrano-Andrés, L.; Shahi, A. R. M.; Gagliardi, L.; Vancoillie, S.; Pierloot, K. *J. Chem. Theory Comput.* **2011**, *7*, 153–168.

(12) Huber, S. M.; Shahi, A. R. M.; Aquilante, F.; Cramer, C. J.; Gagliardi, L. *J. Chem. Theory Comput.* **2009**, *5*, 2967–2976.

(13) Casida, M. E. *Recent advances in Density Functional Methods. Part I*; World Scientific: Singapore, 1995.

(14) Cramer, C. J.; Truhlar, D. G. *Phys. Chem. Chem. Phys.* **2009**, *11*, 10757–10816.

(15) (a) Dreuw, A.; Weisman, J. L.; Head-Gordon, M. *J. Chem. Phys.* **2003**, *119*, 2943–2946. (b) Dreuw, A.; Head-Gordon, M. *Chem. Rev.* **2005**, *105*, 4009–4037.

(16) Neese, F.; Petrenko, T.; Ganyushin, D.; Olbrich, G. *Coord. Chem. Rev.* **2007**, *251*, 288–327.

(17) (a) Ernzerhof, M.; Scuseria, G. E. *J. Chem. Phys.* **1999**, *110*, 5029–5036. (b) Adamo, C.; Barone, V. *J. Chem. Phys.* **1999**, *110*, 6158–6170.

(18) Vydrov, O. A.; Scuseria, G. E. *J. Chem. Phys.* **2006**, *125*, 234109.

(19) (a) Yanai, T.; Tew, D. P.; Handy, N. C. *Chem. Phys. Lett.* **2004**, *393*, 51–56. (b) Peach, M. J. G.; Benfield, P.; Helgaker, T.; Tozer, D. J. *J. Chem. Phys.* **2008**, *128*, 044118.

(20) (a) Jacquemin, D.; Perpète, E. A.; Scuseria, G. E.; Ciofini, I.; Adamo, C. *J. Chem. Theory Comput.* **2008**, *4*, 123–135. (b) Escudero, D.; Trupp, S.; Bussemer, B.; Mohr, G.; González, L. *J. Chem. Theory Comput.* **2011**, *7*, 1062. (c) Jacquemin, D.; Preat, P.; Wathelet, V.; Fontaine, M.; Perpète, E. A. *J. Am. Chem. Soc.* **2006**, *128*, 2072.

(21) (a) Bossert, J.; Daniel, C. *Coord. Chem. Rev.* **2008**, *23*−*24*, 2493–2503. (b) Happ, B.; Escudero, D.; Hager, M. D.; Friebe, C.; Winter, A.; Görls, H.; Altuntas, E.; González, L.; Schubert, U. S. *J. Org. Chem.* **2010**, *75*, 4025–4038. (c) Schulze, B.; Escudero, D.; Friebe, C.; Siebert, R.; Görls, H.; Köhn, U.; Altuntas, E.; Baumgärtel, A.; Hager, M. D.; Winter, A.; Dietzek, B.; Popp, J.; González, L.; Schubert, U. S. *Chem. Eur. J.* **2011**, *17*, 5494. (d) Guthmuller, J.; González, L. *Phys. Chem. Chem. Phys.* **2010**, *12*, 14812–14821. (e) Vlcek, A., Jr.; Zalis, S. *Coord. Chem. Rev.* **2007**, *251*, 258–287.

(22) (a) Petit, L.; Maldivi, P.; Adamo, C. *J. Chem. Theory Comput.* **2005**, *1*, 953–962. (b) Holland, J. P.; Green, J. C. *J. Comput. Chem.* **2010**, *31*, 1008–1014.

(23) Chardon-Noblat, S.; Deronzier, A.; Ziessel, R.; Zsoldos, D. *Inorg. Chem.* **1997**, *36*, 5384–5389.

(24) Eskelinen, E.; Haukka, M.; Venäläinen, T.; Pakkanen, T. A.; Wasberg, M.; Chardon-Noblat, S.; Deronzier, A. *Organometallics* **2000**, *19*, 163–169.

(25) Andrae, D.; Häusermann, U.; Dolg, M.; Stoll, H.; Preuss, H. *Theor. Chim. Acta* **1990**, *77*, 123–141.

(26) (a) Pierloot, K.; Dumez, B.; Widmark, P.-O.; Roos, B. O. *Theor. Chim. Acta* **1995**, *90*, 87. (b) Roos, B. O.; Lindh, R.; Malmqvist, P.-Å.; Veryazov, A.; Widmark, P.-O. *J. Phys. Chem. A* **2005**, *109*, 6575–6579.

(27) (a) Hess, B. A. *Phys. Rev. A* **1985**, *32*, 756. (b) Hess, B. A. *Phys. Rev. A* **1986**, *33*, 3742. (c) Jansen, G.; Hess, B. A. *Phys. Rev. A* **1989**, *39*, 6016.

(28) (a) Aquilante, F.; Pedersen, T. B.; Lindh, R.; Roos, B. O.; De Meras, A. S.; Koch, H. *J. Chem. Phys.* **2008**, *129*, 8. (b) Aquilante, F.; Malmqvist, P. A.; Pedersen, T. B.; Ghosh, A.; Roos, B. O. *J. Chem. Theory Comput.* **2008**, *4*, 694.

(29) Roos, B. O.; Andersson, K.; Fülscher, M. P.; Malmqvist, P. - Å.; Serrano-Andrés, L.; Pierloot, K.; Merchán, M. Multiconfigurational Perturbation Theory: Applications in 35 Electronic Spectroscopy. In *Advances in Chemical Physics: New Methods in Computational Quantum Mechanics*; Prigogine, I., Rice, S. A., Eds.; John Wiley & Sons: New York, 1996; Vol. XCIII, pp 219−332.

(30) Pierloot, K. *Mol. Phys.* **2003**, *101*, 2083–2094.

(31) Pierloot, K. Calculations of electronic spectra of transition metal complexes. In *Computational Photochemistry*; Olivucci, M., Eds.; Elsevier B. V.: Amsterdam, The Netherlands, 2005; pp 279−315.
(32) Finley, J.; Malmqvist, P.-Å.; Roos, B. O.; Serrano-Andrés, L. *Chem. Phys. Lett.* **1998**, *288*, 299.
(33) Malmqvist, P.-Å.; Roos, B. O. *Chem. Phys. Lett.* **1995**, *245*, 215.
(34) Ghigo, G.; Roos, B. O.; Malmqvist, P.-Å. *Chem. Phys. Lett.* **2004**, *396*, 142.
(35) Roos, B. O.; Andersson, K. *Chem. Phys. Lett.* **1995**, *245*, 215.
(36) Roos, B. O.; Malmqvist, P.-Å. *Phys. Chem. Chem. Phys.* **2004**, *6*, 2919.
(37) (a) Becke, A. D. *J. Chem. Phys.* **1993**, *98*, 5648–5652. (b) Lee, C. T.; Yang, W. T.; Parr, R. G. *Phys. Rev. B* **1988**, *37*, 785–789.
(38) Menucci, B.; Cappelli, C.; Guido, C. A.; Cammi, R.; Tomasi, J. *J. Chem. Phys. A* **2009**, *113*, 3009–3020.
(39) Zhao, Y.; Truhlar, D. G. *Theor. Chem. Acc.* **2008**, *215*, 241.
(40) Perdew, J. P.; Burke, K.; Ernzerhof, M. *Phys. Rev. Lett.* **1996**, *77*, 3865–3868.
(41) (a) Cossi, M.; Barone, V.; Menucci, B.; Tomasi, J. *Chem. Phys. Lett.* **1998**, *286*, 253. (b) Menucci, B.; Tomasi, J. *J. Chem. Phys.* **1997**, *106*, 5151.
(42) Frisch, M. J.; Trucks, G. W.; Schlegel, H. B.; Scuseria, G. E.; Robb, M. A.; Cheeseman, J. R.; Scalmani, G.; Barone, V.; Mennucci, B.; Petersson, G. A.; Nakatsuji, H.; Caricato, M.; Li, X.; Hratchian, H. P.; Izmaylov, A. F.; Bloino, J.; Zheng, G.; Sonnenberg, J. L.; Hada, M.; Ehara, M.; Toyota, K.; Fukuda, R.; Hasegawa, J.; Ishida, M.; Nakajima, T.; Honda, Y.; Kitao, O.; Nakai, H.; Vreven, T.; Montgomery, J. A., Jr.; Peralta, J. E.; Ogliaro, F.; Bearpark, M.; Heyd, J. J.; Brothers, E.; Kudin, K. N.; Staroverov, V. N.; Kobayashi, R.; Normand, J.; Raghavachari, K.; Rendell, A.; Burant, J. C.; Iyengar, S. S.; Tomasi, J.; Cossi, M.; Rega, N.; Millam, N. J.; Klene, M.; Knox, J. E.; Cross, J. B.; Bakken, V.; Adamo, C.; Jaramillo, J.; Gomperts, R.; Stratmann, R. E.; Yazyev, O.; Austin, A. J.; Cammi, R.; Pomelli, C.; Ochterski, J. W.; Martin, R. L.; Morokuma, K.; Zakrzewski, V. G.; Voth, G. A.; Salvador, P.; Dannenberg, J. J.; Dapprich, S.; Daniels, A. D.; Farkas, Ö.; Foresman, J. B.; Ortiz, J. V.; Cioslowski, J.; Fox, D. J. *Gaussian 09*, revision A.1; Gaussian, Inc.: Wallingford, CT, 2009.
(43) (a) Karlström, G.; Lindh, R.; Malmqvist, P. -Å.; Roos, B. O.; Ryde, U.; Veryazov, V.; Widmark, P. -O.; Cossi, M.; Schimmelpfennig, P.; Neograd y, P.; Seijo, L. *Comput. Mater. Sci.* **2003**, *28*, 222. (b) Aquilante, F.; De Vico, L.; Ferré, N.; Ghigo, G.; Malmqvist, P.-Å.; Neogrády, P.; Pedersen, T. B.; Pitonak, M.; Reiher, M.; Roos, B. O.; Serrano-Andrés, L.; Urban, M.; Veryazov, V.; Lindh, R. *J. Comput. Chem.* **2010**, *31*, 224.
(44) Vallet, V.; Strich, A.; Daniel, D. *Chem. Phys.* **2005**, *311*, 13.
(45) Daniel, C. *Coord. Chem. Rev.* **2003**, *238−239*, 143–146.
(46) Rosa, A.; Baerends, E. J.; Gisbergen, S. J. A.; Lenthe, E. V.; Groeneveld, J. A.; Snijders, J. G. *J. Am. Chem. Soc.* **1999**, *121*, 10356.
(47) (a) Serrano-Andrés, L.; Fülscher, M. P. *J. Am. Chem. Soc.* **1998**, *120*, 10912. (b) Peach, M. J. G.; Benfield, P.; Helgaker, T.; Tozer, D. J. *J. Chem. Phys.* **2008**, *128*, 044118.
(48) (a) Záliš, S.; Ben Amor, N.; Daniel, C. *Inorg. Chem.* **2004**, *43*, 7978. (b) Ben Amor, N.; Záliš, S.; Daniel, C. *Int. J. Quantum Chem.* **2006**, *106*, 2458.
(49) (a) Peach, M. J. G.; Ruth Le Sueur, C.; Ruud, K.; Guillaume, M.; Tozer, D. J. *Phys. Chem. Chem. Phys.* **2009**, *11*, 4465. (b) Plötner, J.; Tozer, D. J.; Dreuw, A. *J. Chem. Theory Comput.* **2010**, *6*, 2315–2324. (c) Jacquemin, D.; Perpète, A.; Scuseria, G. E.; Ciofini, I.; Adamo, A. *Chem. Phys. Lett.* **2008**, *465*, 226.
(50) Fraser, M. G.; Blackman, A. G.; Irwin, G. I. S.; Easton, C. P.; Gordon, K. C. *Inorg. Chem.* **2010**, *49*, 5180.
(51) Georgieva, I.; Aquino, A. J. A.; Trendafilova, N.; Santos, P. S.; Lischka, H. *Inorg. Chem.* **2010**, *49*, 1634–1646.